

Scalable Clifford-Based Classical Initialization for the Quantum Approximate Optimization Algorithm

Dhanvi Bharadwaj
dhanvib@umich.edu
University of Michigan
Ann Arbor, MI, USA

Guang-Yi Li
lgy@umich.edu
University of Michigan
Ann Arbor, MI, USA

Yuewen Hou
isaachyw@umich.edu
University of Michigan
Ann Arbor, MI, USA

Gokul Subramanian Ravi
gsravi@umich.edu
University of Michigan
Ann Arbor, MI, USA

Abstract

Variational Quantum Algorithms (VQAs), such as the Quantum Approximate Optimization Algorithm (QAOA), offer a promising route to tackling combinatorial optimization problems on near and intermediate-term quantum devices. However, their performance critically depends on the choice of initial parameters, and the limited expressiveness of the QAOA ansatz makes identifying effective initializations both difficult and unscalable. To address this, we propose a framework, Scalable Parameter Initialization for QAOA (SPIQ)¹, that employs a relaxed QAOA ansatz to enable classical search over a set of Clifford-preparable quantum states that yield high-quality solutions. These states serve as superior QAOA initializations, driving rapid convergence while significantly reducing the quantum circuit evaluations needed to reach high-quality solutions and consequently lowering quantum-device cost.

We present a scalable, application-agnostic initialization framework that achieves an absolute accuracy improvement of up to 80% over state-of-the-art initialization and reduces initial-state diversity by up to 10,000 \times across QUBO, PUBO, and PCBO problems spanning tens to hundreds of qubits. We further benchmark its performance on a wide range of problem formulations and instances derived from real-world datasets, demonstrating consistent and scalable improvements. Furthermore, we introduce two complementary strategies for selecting high-quality Clifford points identified by our search procedure and using them to seed multi-start optimization, thereby enhancing exploration and improving solution quality.

1 Introduction

Quantum computers offer the promise of computational advantage, especially in key areas like chemistry [33], optimization [45], and machine learning [4].

Quantum computing is rapidly progressing beyond small-scale, highly noisy NISQ devices [52] toward systems with

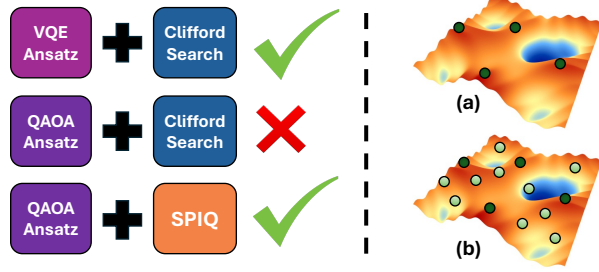


Figure 1. (Left): High-level illustration of how initialization frameworks identify high-quality starting points across variational algorithms. The state-of-the-art Clifford approach (CAFQA) performs well for VQE but fails on standard QAOA due to its extremely limited optimization landscape. In contrast, SPIQ with QAOA yields robust and effective initialization. (Right): (a) Only a few, low-quality Clifford states are found with CAFQA, while (b) our framework, SPIQ, finds many high-quality Clifford points.

thousands of qubits supported by sophisticated error mitigation and potentially lightweight (or partial) error correction techniques [21, 29, 31, 34]. These emerging systems may enable practical utility [35] by executing circuits with a non-trivial number of logical qubits and depths on the order of thousands of gates [31]. However, they will still fall short of supporting long-duration quantum algorithms [23, 60], which require millions of qubits, full fault tolerance, and the ability to perform billions of quantum operations [50].

There are certain algorithms that exhibit an innate robustness to noise, allowing them to generate valuable results even without full fault tolerance. Among these, Variational Quantum Algorithms (VQAs) [8] are especially notable for their broad applicability. There is optimism within the community [71] that we should continue to advance them in the hope of achieving real-world utility on next-generation quantum systems in areas such as combinatorial optimization [14], physics [35], and chemistry [51]. VQAs are hybrid

¹SPIQ (pronounced “spike”) will be open-sourced.

algorithms in which a parameterized quantum circuit is iteratively refined by a classical routine. Over time, the VQA explores the quantum solution landscape, minimizing an objective function to converge on the problem’s “ground state”, i.e., the optimal solution.

Within the broader class of VQAs, one algorithm specifically designed to approximately solve combinatorial optimization problems is the Quantum Approximate Optimization Algorithm (QAOA) [14]. QAOA alternates between applying problem-specific and mixing Hamiltonians, with the goal of steering the parameterized state toward a low-energy state that encodes a high-quality solution. The algorithm is parameterized by a set of a few angles that define the rotation gates, which are tuned by a classical optimizer to minimize the expectation value of the final quantum state. As the circuit depth (p) increases, QAOA can, in principle, approximate the optimal solution with increasing accuracy, making it a promising candidate for near-term quantum advantage in discrete optimization tasks.

As with many optimization algorithms, the choice of initial parameters in QAOA strongly influences solution quality, and good initialization can substantially reduce quantum and classical resource costs by cutting the number of required circuit evaluations and improve the accuracy of the converged solution [5, 57]. However, searching for these low-energy initial parameters, especially in high-dimensional and noisy landscapes, is computationally intensive. This challenge is amplified when evaluations must be performed on actual quantum hardware, where each function call may require numerous circuit executions (shots), making the process resource- and time-consuming. Previous initialization strategies for QAOA have largely been tailored to specific problem instances [64, 67, 69], often relying on domain-specific knowledge or heuristics. Furthermore, many of these methods have typically been tested only on unconstrained or small-scale problems and on unweighted graph instances, and have not demonstrated effectiveness at larger scales.

To the best of our knowledge, there is currently no general-purpose initialization framework that is both broadly applicable and scalable across diverse problem types. These limitations pose a significant barrier to the widespread and efficient deployment of QAOA across the full spectrum of combinatorial optimization problems [42], including Quadratic Unconstrained Binary Optimization (QUBO), Polynomial Unconstrained Binary Optimization (PUBO), and Polynomial Constrained Binary Optimization (PCBO).

To find a promising initialization strategy for the QAOA, we look to the initialization landscape of another VQA, the Variational Quantum Eigensolver (VQE) [51]. Among many techniques, VQE has particularly benefited from scalable and classically simulable strategies based on Clifford states [55]. That framework, CAFQA, demonstrates strong performance on quantum chemistry tasks and highlights the value of high-quality initializations for improving convergence and

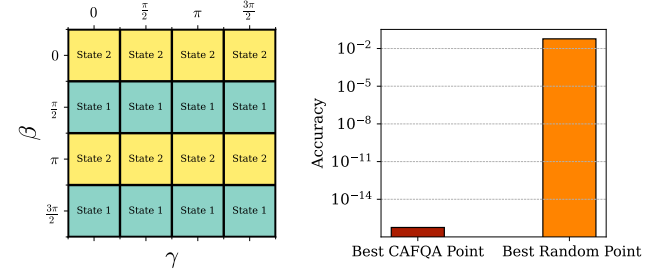


Figure 2. (Left): Heatmap of unique Clifford states found by CAFQA, with both states yielding expectation values ≈ 0 , indicating that only a few states are explored and resulting in low-quality solutions. (Right): Comparison of best energies, showing that a random guess (best of 50) can outperform CAFQA initialization for QAOA.

solution quality. However, directly applying this strategy to QAOA is ineffective because of the QAOA circuit’s highly constrained structure. In particular, the limited expressiveness of the QAOA ansatz prevents it from representing a high-quality stabilizer state [9].

We illustrate this limitation in Fig. 2 using a weighted Max-Cut instance on a 10-node complete graph, a typical QAOA toy problem. For a QAOA circuit with depth $p = 1$, the CAFQA search space contains only $(2p)^4 = 16$ Clifford angle combinations. We classically evaluate the expectation value (or ‘energy’) of each candidate Clifford point. The resulting discrete heatmap clearly shows that the CAFQA-reachable points lie in a low-quality region of the landscape. To contextualize this, we compare against the best initialization from 50 random starts and report the *accuracy*, here defined as the closeness of the initialization energy to the true classical optimum. CAFQA performs significantly worse than random initialization because the restricted Clifford parameter space available to QAOA provides too few high-quality candidates. This highlights a fundamental limitation of directly applying Clifford-based initialization strategies to QAOA. To overcome the limitations of Clifford-based QAOA initialization described above, we instead seek to leverage a fundamentally orthogonal QAOA strategy, which we describe next.

While increasing the ansatz depth theoretically enhances the expressivity of the QAOA circuit [14], deeper circuits suffer from amplified noise on current hardware, which quickly degrades state fidelity [46, 65]. Even on early fault-tolerant systems [12, 34], added depth is undesirable due to the increased number of rotational gates and corresponding resource overhead. These challenges have motivated advances in ansatz design. Among them, Multi-Angle QAOA (ma-QAOA) [28] introduces a more expressive QAOA circuit structure that allows independent rotation angles within each layer without increasing circuit depth.

Inspired by this approach, we find that relaxing the correlation between QAOA circuit parameters substantially *improves the circuit’s capacity to generate high-quality Clifford states* on classical compute, providing a pathway to effective and scalable QAOA initialization. Building on this insight, we propose a versatile initialization framework that leverages the relaxed-parameter ansatz together with a Clifford-based search strategy to efficiently identify near-ground-state solutions classically. To further mitigate the risk of initializing near non-convex regions, we introduce two strategies that select Clifford initialization points from diverse regions, enabling a multi-start procedure that promotes broader landscape exploration, typically avoids local minima, and increases the likelihood of high-quality solutions. Fig. 1 provides a high-level overview of our approach. Unlike existing initialization methods tailored to specific problems, our method applies broadly to diverse combinatorial optimization tasks, yielding a scalable and versatile QAOA framework suitable for all quantum computers from today’s NISQ devices to tomorrow’s EFT systems.

The primary contributions and insights of our work are:

1. We develop **SPIQ** - a scalable, Clifford-driven initialization framework for QAOA. SPIQ overcomes the poor QAOA performance of traditional VQE-style Clifford techniques and generalizes effectively across diverse combinatorial optimization problems, without requiring problem-specific heuristics.
2. We leverage the expressive structure of ma-QAOA [28], demonstrating that beyond reducing circuit depth, it provides an effective framework for exploring and identifying high-quality Clifford states, with its expressivity naturally scaling with problem size and capturing richer structure in complex instances.
3. We demonstrate that high-quality Clifford initialization prunes the QAOA solution space, eliminating a large fraction of non-optimal states.
4. We introduce a gradient norm-based technique to strategically select high-quality Clifford points from different regions of the landscape to seed a multi-start optimization that mitigates non-convexity and device noise, and increases the likelihood of reaching high-quality solutions.
5. Our evaluations across diverse QUBO and PCBO instances (including real-world datasets) show that the proposed approach consistently outperforms existing warm-start methods and attains up to 99.9% of the optimal solution, demonstrating strong robustness and generalization.

2 Background & Motivation

2.1 Combinatorial Optimization Problems

Combinatorial optimization lies at the heart of many real-world decision-making, where the objective is to find the

best solution from a finite but often exponentially large set of possibilities. These problems arise in diverse fields such as logistics [58], finance [49], and operations research [54]. Formally, a combinatorial optimization problem involves selecting a subset or ordering of discrete variables that maximizes a given cost function under certain constraints. Despite their simplicity in formulation, these problems are often NP-hard, making them computationally challenging for classical algorithms as problem sizes scale. We focus on two problem classes: QUBO and PCBO. QUBO has a quadratic objective over binary variables with no explicit constraints, while PCBO involves polynomial objectives with algebraic or logical constraints, making it more expressive but computationally harder.

On classical computers, these problems are traditionally solved using a combination of exact and heuristic methods. Exact approaches such as branch-and-bound, branch-and-cut, and semidefinite relaxations, implemented in solvers like CPLEX and Gurobi [25, 30], can provide optimal solutions but quickly become intractable as problem sizes grow due to exponential scaling. To handle larger instances, a wide range of heuristics, including simulated annealing and genetic algorithms, are employed to find high-quality approximate solutions [7]. PCBO problems are often reduced to equivalent QUBO instances through quadratization techniques [2, 6], enabling the use of the same solver ecosystem but at the cost of introducing additional variables and constraints. Consequently, for both QUBO and PCBO, practical scalability hinges on heuristics and approximation strategies [20, 37].

2.2 Quantum Approximate Optimization Algorithm (QAOA)

The Quantum Approximate Optimization Algorithm (QAOA) is a hybrid quantum-classical algorithm tailored for solving combinatorial optimization problems. At its core, QAOA constructs a parameterized quantum circuit composed of alternating p layers of problem-specific and mixing unitaries, each controlled by a set of classical parameters.

In QAOA, an optimization problem is encoded into a cost Hamiltonian H_C and paired with a mixer Hamiltonian H_M to guide the variational evolution. The unitary operators $U(\gamma, H_C) = e^{-iH_C\gamma}$ and $U(\beta, H_M) = e^{-iH_M\beta}$, with variational parameters γ and β , are applied alternately for p repetitions to evolve an initial quantum state towards low-energy configurations of H_C . The circuit is initialized in the uniform superposition of all computational basis states, $|s\rangle = \frac{1}{\sqrt{2^n}} \sum_z |z\rangle$. This construction is referred to as the traditional QAOA ansatz.

QAOA relies critically on the choice of variational parameters $(\vec{\gamma}, \vec{\beta})$, which control the depth- p quantum evolution. Optimizing these parameters is challenging due to the non-convexity and instance-specific structure of the cost landscape [3, 10, 13, 15, 26, 27, 41, 43, 63, 66]. These challenges

arise, in part, from fundamental differences between QAOA and other variational algorithms, such as the Variational Quantum Eigensolver (VQE).

While QAOA shares structural similarities with VQE, it targets discrete optimization over classical cost functions rather than ground-state estimation. Its layered, problem-specific ansatz constrains expressivity, making performance highly sensitive to parameter initialization. Increasing the circuit depth (p) can enhance expressivity but also amplifies noise, further complicating optimization. Together, these factors underscore the importance of principled initialization strategies to efficiently guide QAOA toward high-quality solutions.

Addressing these challenges starts with carefully formulating the optimization problem, as its representation affects QAOA circuit design and parameter initialization. Problem instances are generated in QUBO, PUBO, or PCBO form, expressing the objective function with binary variables and polynomial cost terms suitable for quantum optimization. A general QUBO problem is expressed as minimize $x^T Qx$, where $x \in \{0, 1\}^n$ and $Q \in \mathbb{R}^{n \times n}$ is a real-valued symmetric matrix. A PUBO extends this to higher-order terms: minimize $\sum_i a_i x_i + \sum_{i < j} b_{ij} x_i x_j + \sum_{i < j < k} c_{ijk} x_i x_j x_k + \dots$. A PCBO introduces equality or inequality constraints on binary variables: minimize $f(x)$ subject to $g_k(x) = 0$, $h_l(x) \leq 0$, where $f(x)$ is a polynomial objective and g_k, h_l are polynomial constraint functions.

2.3 Parameter Relaxed Ansatz for QAOA

The standard QAOA ansatz is minimally parameterized, typically using only $2p$ parameters. For increasing expressivity as the problem size grows, one could increase the number of classical parameters per QAOA layer. This is achieved by leveraging the multi-angle QAOA (ma-QAOA) [28], which enhances the traditional structure by assigning individual parameters to each term in the cost and mixer operators, instead of using a single angle for each. Specifically:

$$U(H_C, \vec{\gamma}_\ell) = e^{-i \sum_{a=1}^m H_{C,a} \gamma_{\ell,a}} = \prod_{a=1}^m e^{-i H_{C,a} \gamma_{\ell,a}},$$

$$\text{and } U(H_M, \vec{\beta}_\ell) = e^{-i \sum_{b=1}^n H_{M,b} \beta_{\ell,b}} = \prod_{b=1}^n e^{-i H_{M,b} \beta_{\ell,b}}.$$

Here, m is the number of clauses and n is the number of qubits. The total number of parameters becomes $(m + n) * p$. The standard QAOA is a special case of ma-QAOA, where all parameters within a cost or mixer layer are identical. ma-QAOA expands the parameter space, allowing the exploration of more complex solution landscapes and improves optimization efficiency. The difference in ansatz structure between the traditional QAOA and ma-QAOA is illustrated in Fig. 3.

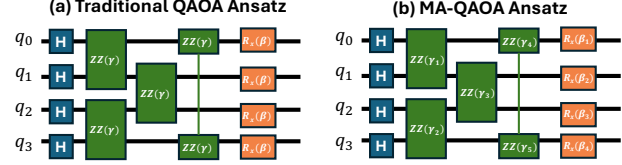


Figure 3. Structural differences between a $p = 1$ (a) traditional QAOA ansatz and the (b) Multi-Angle QAOA ansatz

2.4 Clifford-Based Initialization in Variational Quantum Eigensolver

Clifford gates form a fundamental class of quantum operations that map Pauli operators to Pauli operators under conjugation, making circuits composed of them efficiently simulable on classical hardware [22]. This property allows structured exploration of large, yet tractable, regions of the Hilbert space and makes Clifford states attractive as high-quality starting points for variational algorithms. Prior work, such as Clifford Ansatz For Quantum Accuracy (CAFQA) [55], has leveraged this principle to enhance VQE performance. By initializing with Clifford states, CAFQA narrows the optimization landscape, achieving high overlap with the true ground state and demonstrating remarkable accuracy in quantum chemistry tasks. These successes highlight both the potential and limitations of Clifford-based initialization: while they provide strong heuristic starting points, their effectiveness depends critically on the expressivity of the underlying ansatz. Unlike VQE, the QAOA employs a fixed, layered ansatz of alternating unitaries generated by the cost Hamiltonian H_C and a non-commuting mixer Hamiltonian H_M . This constrained ansatz limits the reachable state space and poses challenges for integrating pre-optimized Clifford states. Hence, methods like CAFQA have been largely confined to VQE domains and have not been applied to combinatorial optimization problems.

2.5 Importance of Initialization in QAOA

The success of the Quantum Approximate Optimization Algorithm (QAOA) depends heavily on choosing the right starting values for its variables [5, 57]. Without proper initialization, the algorithm often gets stuck in poor local minima or faces "barren plateaus" where it cannot find the right direction to improve the solution [39]. To address this, researchers use specific techniques like **INTERP**, which builds complex circuits using patterns from simpler ones [69], or **TQA**, which mimics a natural quantum annealing process [57]. However, these methods face significant limitations as they are often problem-specific and do not scale well, requiring costly custom adjustments as the complexity of the task changes. This lack of a general, scalable approach remains a major barrier to using QAOA for diverse, real-world applications.

2.6 Red-QAOA

As the problem size grows, larger circuits amplify noise and distort the optimization landscape. Red-QAOA [64] addresses this by using simulated-annealing-based graph reduction to identify smaller, structurally equivalent graphs, allowing the parameter-search phase to run on shallower, less noise-sensitive circuits. The resulting parameters are then transferred back to the full graph as high-quality initialization points.

While producing encouraging results, Red-QAOA is fundamentally graph-centric, limiting it to problems with natural graph representations. Reformulating non-graph or higher-order problems is nontrivial. The method also incurs quantum resource overhead by requiring execution of both reduced and full circuits. Additionally, landscape-preservation guarantees weaken for weighted graphs, where structured edge weights can degrade solution quality. These constraints highlight the need for scalable, problem-agnostic classical initialization strategies.

2.7 Iterative VQA Optimization

Once initialized, QAOA pursues iterative optimization on the quantum device. For this, one could flexibly choose from a variety of classical optimizers depending on the problem characteristics. Gradient-free optimizers such as COBYLA [68], SPSA [62], and Nelder-Mead [19] are often preferred in noisy or non-smooth landscapes, while gradient-based optimizers like L-BFGS-B [70] and Adam [36] can offer faster convergence when gradient information is reliable.

Each classical optimizer instance repeatedly updates the variational parameters $(\vec{\gamma}, \vec{\beta})$ of the quantum circuit, improving the solution and maximizing the cost function based on quantum measurement outcomes. This continuous optimization process is not limited to discrete Clifford angles; it allows any angle in the interval $[-\pi, \pi]$, expanding the search beyond the Clifford subspace. The iterative optimization continues until convergence, or it is terminated early upon reaching a predetermined iteration cap to constrain quantum resource consumption.

2.8 Post-Processing

After classical optimization, QAOA produces a quantum state $|\psi(\vec{\gamma}, \vec{\beta})\rangle = U_{\text{QAOA}}(\vec{\gamma}, \vec{\beta})|0\rangle$, which is measured in the computational basis to yield bitstrings \mathbf{z} with probabilities $P(\mathbf{z}) = |\langle \mathbf{z} | \psi(\vec{\gamma}, \vec{\beta}) \rangle|^2$. The most probable bitstring, often determined via repeated sampling, is selected as the candidate solution. For combinatorial problems, bitstrings are interpreted according to problem structure. In Max-Cut, bits assign vertices to partitions maximizing edges between sets [14]; in knapsack-like problems, bits indicate selected items while respecting constraints [11]. Post-processing thus ensures feasible, high-quality solutions tailored to each problem.

2.9 Multi-Start Optimization Strategies

In complex, non-convex optimization landscapes such as those encountered in QAOA, the algorithm's performance is often highly sensitive to the initial parameter choice. A single optimization run, even from a well-chosen warm-start point, risks converging to a sharp or undesirable local minimum [40, 57]. A multi-start optimization strategy [56] mitigates this risk by launching multiple independent runs from a diverse set of initial points, or seeds, and selecting the best result. In this work, we develop two strategies for selecting high-quality starting points to maximize exploration and improve convergence through multi-start.

3 End-to-End Workflow

We propose a framework that leverages the expressive solution space enabled by the ma-QAOA ansatz to efficiently search for high-quality Clifford states as high-quality initialization points. The following subsections describe each component of the framework in detail, and the framework is illustrated in Fig. 4. At a high level, the important steps in the QAOA workflow are:

1. **Generate Problem Instance:** Formulate the optimization problem as a QUBO or PCBO instance and map it to a Hamiltonian, where the ground state corresponds to the optimal solution of the original cost function.
2. **Build ma-QAOA Ansatz:** Create a multi-angle ansatz which will prepare the ground state of this Hamiltonian.
3. **Search Clifford Space for Initial Parameters:** Perform a classical search for high-quality Clifford parameters for $(\vec{\gamma}, \vec{\beta})$.
4. **Strategic Selection of Clifford Points:** Strategically choose Clifford initialization points from different regions to seed a multi-start optimization, improving exploration, avoiding local minima, and increasing the likelihood of high-quality solutions.
5. **Optimize from Selected Points:** Initialize the QAOA ansatz with the chosen Clifford states and perform classical optimization of the variational parameters to iteratively minimize the cost function, refining the solution toward high-quality optima.
6. **Post-Process:** Sample the final quantum state to extract the most probable bitstring, and the resulting output is interpreted as a solution for the original optimization problem.

Steps 1, 5, and 6 align with the standard QAOA workflow; further details appear in Section 2, where we outline the conventional QAOA process. In this section, we present the core components of SPIQ.

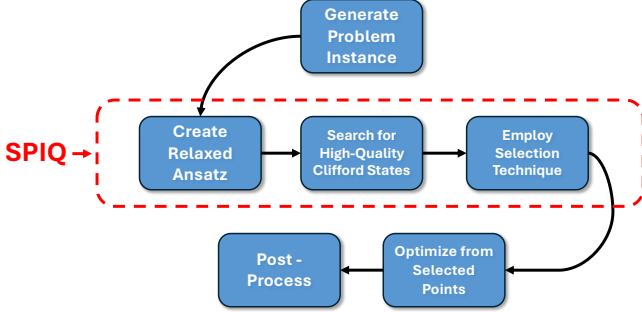


Figure 4. Overview of the QAOA + SPIQ workflow

3.1 Relaxed Ansatz

Once the cost Hamiltonian is constructed, it forms the foundation for building the QAOA ansatz, which governs the evolution of the quantum state. To enhance the ansatz’s expressiveness, we employ the ma-QAOA structure. We start by constructing a standard QAOA ansatz using Qiskit’s QAOAAnsatz API [32], which provides the traditional $2p$ -parameter ansatz. We then relax the parameters $(\vec{\gamma}, \vec{\beta})$, allowing them to vary independently and increasing flexibility. This results in a total of $(m + n) * p$ parameters, where m is the number of clauses and n is the number of qubits. The ma-QAOA structure is illustrated in Fig. 3(b).

3.2 Clifford Search

We leverage the ma-QAOA structure as it offers a broader solution space for exploring high-quality Clifford states. Recall that this process is entirely classical since the execution of Clifford-only circuits only requires polynomial time [22]. We then utilize a discrete search technique to explore Clifford angle parameters that minimize the expectation value of the quantum circuit with respect to the cost Hamiltonian. To perform this search, we leverage a gradient-free Genetic Algorithm (GA) [1] optimizer to navigate the Clifford solution space. While any discrete optimizer can be used, we choose GA since it offers substantial parallelism: each individual in a generation can be generated independently, making every generation fully parallelizable.

The GA is implemented using the PyGad library [17]. Since these parameters dictate the angles in the rotational gates of the ansatz, they can only take values that are integer multiples of $\frac{\pi}{2}$, corresponding to rotations by $0, \frac{\pi}{2}, \pi$, or $\frac{3\pi}{2}$ radians. These specific angles ensure that the quantum operations remain within the Clifford group, which is efficiently simulable and preserves Pauli operators under conjugation.

3.3 Strategic Selection of Clifford points

Because the Clifford search is agnostic to the surrounding landscape, the lowest-energy Clifford state may still lie near a sharp local minimum or barren plateau, which can hinder

QAOA tuning. A multi-start optimization strategy [56] mitigates this risk by launching several independent optimization runs from diverse seeds and retaining the best solution across them. The performance of the multi-start strategy is critically dependent on the method used to select these seeds. To address this, we introduce two complementary strategies for selecting high-quality, landscape-aware seeds that reliably strengthen the search from different regions of the landscape.

Our first strategy is the *Fixed-Interval Selection* method, which orders candidates by expectation value and picks points at regular intervals along this sorted list. This offers a direct way to highlight promising candidates while maintaining broad coverage. While this method ensures diversity in expectation value, it ignores the geometric structure of the parameter space, and the selected points may still be clustered in the same basin of attraction or reside in a stationary region, where a subsequent optimization algorithm cannot easily find a path for improvement [38].

To address this, we introduce a second method, *K-GAPS* (K-means Gradient-Aware Point Selection), that leverages K-means clustering and gradient-norm heuristics to identify effective Clifford states.

First, K-means clustering [61] is utilized to ensure spatial diversity. As an unsupervised algorithm, K-means partitions the candidate solutions into k clusters based on *distance* in the high-dimensional parameter space, ensuring that the selected seeds lie in structurally distinct regions.

A key aspect of our approach is how we define distances between seed points. Each coordinate of a seed corresponds to a VQA circuit parameter, which is a *circular angle* in $[0, 2\pi)$ (for Clifford states, $0, \frac{\pi}{2}, \pi, \frac{3\pi}{2}$). If we cluster raw angles directly, points like 0 and $2\pi - \varepsilon$ appear far apart, even though they represent nearly identical states. To address this, we embed each angle θ onto the unit circle as $(\cos \theta, \sin \theta)$, capturing its periodicity. We then apply K-means to these 2D embeddings for every parameter, producing distances that meaningfully reflect the geometry of the VQA parameter space. Although each of these components (angle embedding, geometric distance, and clustering) can be considered separately, we combine them to effectively select diverse and representative seed points for our use case.

Second, the gradient norm is used to filter for optimization potential. The gradient norm quantifies the steepness of the landscape at a point θ . For a function f with n parameters $\theta = (\theta_1, \dots, \theta_n)$, this is typically the L2-norm [48], defined as:

$$\|\nabla f(\theta)\|_2 = \sqrt{\sum_{i=1}^n \left(\frac{\partial f}{\partial \theta_i}\right)^2}$$
 For a function that is an output of a variational quantum circuit, these partial derivatives are computed via the parameter-shift rule [44], e.g., for a single parameter θ_j ,

$$\frac{\partial f}{\partial \theta_j} = \frac{1}{2} \left[f(\theta_1, \dots, \theta_j + \frac{\pi}{2}, \dots, \theta_n) - f(\theta_1, \dots, \theta_j - \frac{\pi}{2}, \dots, \theta_n) \right],$$
 with shifts of $\pm \frac{\pi}{2}$. Crucially, since the candidate seeds are

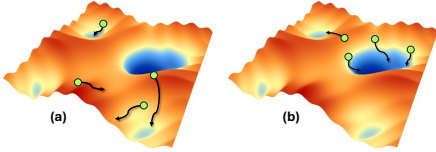


Figure 5. Illustration comparing two strategies for selecting points from high-quality SPIQ states: (a) naive selection may get stuck in local minima or barren plateaus, (b) choosing diverse points near steep curves helps avoid non-convex regions.

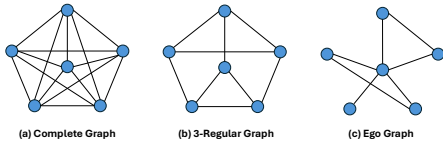


Figure 6. Illustration of graphs used for Max-Cut with 6 nodes as an example: (a) Each node is connected to every other node. (b) Each node is connected to exactly three other nodes. (c) Central node and its neighbors.

Clifford states, these shifts of $\pm \frac{\pi}{2}$ ensure the circuits remain within the Clifford group, enabling rapid gradient evaluation via efficient stabilizer simulation [22]. A near-zero norm indicates that a point is already in a stationary region, such as a plateau or local minimum, making it a poor seed for subsequent optimization. Fig. 5(b) illustrates the selection of points using this approach, which ensures seeds are both high-quality and spatially diverse, with strong potential for further variational improvement.

4 Methodology

To systematically evaluate the performance of our framework, we use one QUBO problem and two PCBO problems as benchmarks for QAOA.

4.1 Benchmarks

4.1.1 QUBO Benchmark. We select Max-Cut as the QUBO benchmark. The cost Hamiltonian for a graph G with edge set $E(G)$ is typically expressed as $H_C = \sum_{(i,j) \in E(G)} \frac{1}{2} w_{ij} (I - Z_i Z_j)$, where w_{ij} are the edge weights and Z_i, Z_j are Pauli-Z operators acting on qubits corresponding to nodes i and j .

Max-Cut provides a suitable testbed for our framework, allowing exploration of diverse graph structures under consistent optimization settings. We evaluate performance on three graph types, illustrated in Fig. 6: Complete graphs, 3-Regular graphs, and Ego graphs. Complete graphs are densely connected, creating a highly entangled optimization landscape, while 3-Regular graphs are sparsely connected, with each node linked to three others, producing more localized interactions. Ego graphs, built around a central “ego” node and its neighbors, capture intermediate connectivity and local

community structure. Weighted graph instances are generated by randomly assigning integer edge weights between 0 and 10, enabling assessment across diverse input conditions.

4.1.2 PCBO Benchmarks. We select the Knapsack problem and a medical high-order interaction problem [59] as representative PCBO benchmarks. The Knapsack problem is encoded as a PUBO Hamiltonian using the Qiskit Optimization module [53], incorporating penalty terms to enforce the weight constraint. Random instances are generated with appropriate item weights and values to create meaningful optimization challenges. For the medical high-order interaction benchmark [59], each variable represents a gene-associated measurement, with bits indicating inclusion in the subset. The PCBO formulation captures both individual relevance and higher-order dependencies (pairwise and triple-wise mutual information) between measurements and outcomes, represented as a hypergraph with weighted edges. The goal is to select M measurements from N variables to maximize relevance while minimizing redundancy, enforced via a Hamming-weight constraint with a Lagrange penalty.

4.2 Evaluation Metrics

The primary metric used in this work is *Accuracy*, which quantifies the quality of our initialization relative to the true ground state. We define accuracy as $\text{Accuracy} = \frac{E_{\text{init}}}{E_{\text{opt}}}$, where E_{init} is the objective value of the initial state provided by different techniques, and E_{opt} is the objective value of the optimal ground state. A higher accuracy indicates that the initialization produces a state closer to the true optimum, likely serving as a more effective starting point for subsequent QAOA optimization.

In addition to accuracy, we introduce the *Search Space Reduction Factor (SSRF)*, or *Reduction Factor (RF)* for short, to quantify the reduction in the number of solution states between initial points. Specifically, this metric captures how concentrated the quantum state becomes after initialization, by comparing the number of unique bitstrings sampled. We define $\text{RF} = \frac{N_{\text{random}}}{N_{\text{init}}}$, where N_{random} is the number of distinct bitstrings observed when sampling from a randomly initialized ma-QAOA ansatz, and N_{init} is the number of distinct bitstrings observed after applying our initialization framework. All measurements are performed using the same total number of shots. A higher RF indicates that the initialized state is more sharply concentrated over a smaller portion of the solution space, enabling more focused and efficient exploration during QAOA optimization.

For large-scale problem instances where the true ground state energy is intractable to compute, we introduce *Relative Improvement* to quantify the effectiveness of initialization, defined as $\text{Relative Improvement} = E_{\text{init}}/E_{\text{rand}}$, where E_{init} is the objective value of the state obtained from our Clifford-initialized framework, and E_{rand} is the objective value of a randomly initialized state. A higher relative improvement

indicates that the Clifford initialization provides a better starting point for optimization, guiding the algorithm toward lower-energy regions even when the exact solution is unavailable.

While no single metric fully captures QAOA performance, the chosen metrics effectively assess initialization quality, the scalability of finding high-value starting points, and potential post-initialization tuning.

4.3 Baseline and Evaluation Settings

For this study, we use two baselines: standard QAOA with random parameter initialization and Red-QAOA [64], a warm-start method applicable only to graph problems like Max-Cut (Section 5.4). For our Clifford search and tuning evaluations, we ran simulations on Perlmutter’s [47] CPU node, equipped with AMD EPYC 7763 processors, with a maximum wall clock time of 48 hours per job.

We compare its performance against alternative techniques, including the ma-QAOA ansatz with random initialization, across varying experimental conditions. We design our ma-QAOA ansatz with two repeating layers, corresponding to a depth of $p = 2$. To assess the performance of these methods, we first create a QAOA ansatz with an input Hamiltonian using the Qiskit library [32] and then free the parameters in each layer to be independent, to create the relaxed ma-QAOA ansatz. For noiseless simulations, we use Qiskit’s StatevectorSimulator to obtain exact quantum states. For noise studies, we apply depolarizing noise channels [16] to gates, resets, and measurements.

For our evaluation described in Subsection 5.5, we use Qiskit’s COBYLA optimizer [68] to explore the solution space. Additionally, we showcase the top-performing points for multi-start optimization, selected from both the Fixed-Interval and K-GAPS methods. These evaluations allow us to assess the robustness of each initialization method and ansatz under practical constraints.

5 Evaluation

5.1 Initialization Performance across Benchmarks

We first assess the performance of our initialization strategy across the benchmark combinatorial optimization problems detailed in Section 4.1, as visualized in Figures 7, 8, and 9. We present the initialization accuracies that are computed relative to the ground state energy of the Hamiltonian associated with each combinatorial problem.

5.1.1 Max-Cut Problem on Complete, 3-Regular, and Ego Graphs. In this section, we evaluate the quality of the high-quality initialization point generated by our framework for the ma-QAOA ansatz applied to three distinct graph types in the Max-Cut problem. More information on Max-Cut and the types of graph benchmarks is discussed in Subsection 4.1.1.

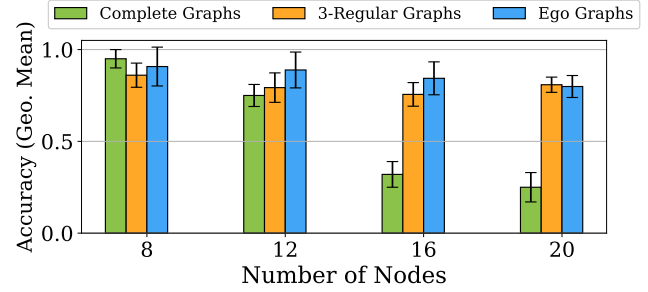


Figure 7. SPIQ Accuracy evaluated on Max-Cut problems for various weighted graphs.

Fig. 7 presents the initialization accuracies for each graph type across different numbers of qubits. We calculate the geometric mean over 10 weighted Max-Cut instances per graph type. In our weighted graphs, edges are assigned weights that modify the optimization objective to account for their relative importance rather than treating all edges equally. When running our initialization framework, we allowed the genetic algorithm optimizer to run for up to 48 hours. In practice, however, most instances converged well before this limit.

We see that the Clifford initialization technique can find strong initialization points for diverse graph structures and sizes. Among the tested graphs, the Clifford initialization consistently achieves high proximity to the true ground state energy, suggesting it provides a strong starting point for optimization. The highest accuracy we achieve is 99.9% for the 3-Regular and Ego graphs, which have fewer edges between the nodes as compared to Complete Graphs. The geometric mean accuracy decreases more starkly for the complete graphs as the number of nodes increases. This is expected as the edges between the nodes increase quadratically with the number of nodes, which makes the landscape extremely difficult to navigate. An increase in the number of edges directly translates to a larger set of $R_{X/Z}(\theta)$ gates in the QAOA ansatz, which enlarges the optimization space and makes the training process more challenging. We note that there are pre-processing techniques [64] to further improve the quality of initialization that we don’t explore in our work.

5.1.2 Knapsack Problem. Next, we assess initialization accuracy on a harder subclass of combinatorial optimization problems, PCBO (see Subsection 4.1.2), using the Knapsack problem as a representative example. In this section, we evaluate the impact of Clifford-based initialization on solving three representative Knapsack problem instances. We generate random 4, 9, and 12-item problems, chosen specifically to align with the number of qubits used in other QUBO and PCBO benchmarks once the problems are translated into Hamiltonian form. This enables consistent comparisons across problem classes. As with the Max-Cut case, we set a

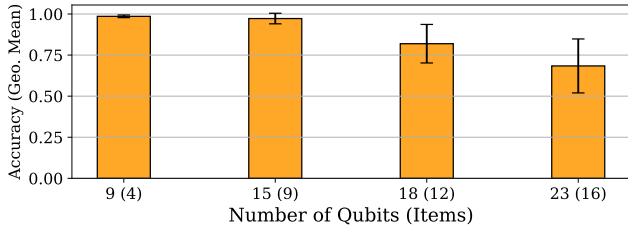


Figure 8. SPIQ Accuracy evaluated on Knapsack problems

48-hour wall time limit; however, most Knapsack runs finished well before this, indicating efficient convergence from the initial point.

Fig. 8 presents the quality of the initial solution from Clifford initialization across four spaced-out problem sizes. We again find that Clifford initialization yields strong overlap with the ground state, demonstrating its effectiveness even before any quantum optimization is performed. In the 4-item case (9 qubits), SPIQ recovers 99.9% of the true energy on average. For the 9-item instance (15 qubits), it retains 98.2% of the ground state energy. Although performance slightly decreases in the largest case (12 items, 18 qubits), recovering 70.2% on average, this result demonstrates that the initialization strategy remains effective at producing low-energy configurations that are still significantly correlated with the ground state, even in high-dimensional, constrained Hamiltonians. The observed trend reflects the increasing difficulty of the optimization problem as the number of parameters grows, though longer runs of the Clifford search (or with more parallelized compute resources) can mitigate this, as discussed in Subsection 6.

5.1.3 Medical High-Order Interaction Benchmark. In this section, we evaluate the Clifford initialization by applying it to a real-world medical biology challenge: selecting maximally informative yet non-redundant gene subsets from high-dimensional genomic data. We can frame the feature selection task as a PCBO problem. The objective function, whose formulation is described in Subsection 4.1.2, creates a non-submodular optimization landscape that tests QAOA’s ability to handle highly constrained combinatorial problems. In our evaluations, we convert the PCBO object, which is represented as a hypergraph, into an Ising Hamiltonian formulation with the process described in Subsection 4.1.2. In our study, the problems are subject to the constraint of choosing exactly 4 features out of the N total features in the datasets.

The benefits of Clifford-based initialization on this problem are illustrated in Fig. 9. The best-performing SPIQ-initialized point achieves a remarkably high 94% accuracy, indicating close recovery of the ground state. While there is a decrease in performance as the number of qubits increases, the initialization strategy continues to yield high-quality solutions, maintaining strong accuracy even in complex landscapes.

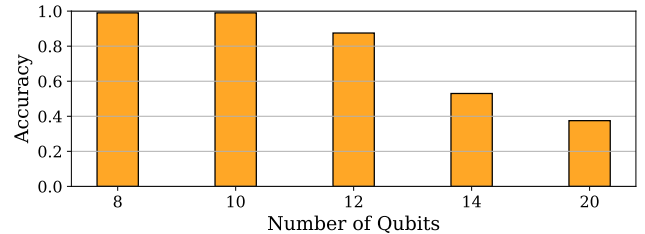


Figure 9. SPIQ evaluated on Medical High-Order Interaction

We also note that these numbers can be boosted with tailored computational techniques and increased run time of the genetic algorithm. These results demonstrate the value of SPIQ in steering the optimizer toward high-fidelity solutions, even as the problem complexity increases.

Together, these results demonstrate that leveraging the expressiveness of ma-QAOA to perform Clifford search significantly improves the solution quality of the initial point. This approach reliably finds near-optimal solutions even in complex, structured optimization problems like those arising in molecular biology. Once again, we note that our current estimates are based on a maximum of 48 hours of runtime, but they can be improved with increased memory or compute resources, extended execution time, improved search heuristics, more efficient parallelization, or targeted exploration beyond Clifford space, as discussed in Subsection 6.

5.2 Scaling to Larger Problem Instances

To assess the scalability of our initialization framework, we apply it to larger problem instances. Specifically, we evaluate performance on Max-Cut problems defined over 10 instances of 3-regular graphs with sizes ranging from 50 to 800 qubits, representing a challenging yet structured class of combinatorial optimization problems.

To quantify the effectiveness of initialization at this scale, we compute the relative improvement, defined as the ratio between the energy of our Clifford-initialized state and that of a randomly initialized state. As shown in Fig. 10, our method achieves significantly better starting points, with improvements reaching up to $10,000\times$ over random initialization. We report results for two exploration strategies: ‘Full Exploration’ shows the best Clifford state identified after running the search up to the 48-hour maximum wall time, while ‘Minimal Exploration’ indicates the first state found among all generations within the same wall-time limit, highlighting that even limited exploration can produce high-quality states at scales beyond the reach of other classically simulable initialization techniques.

These results underscore the importance of informed initialization for steering the optimizer toward low-energy regions, even in large problems. Large initial gains reduce the quantum optimization burden, benefiting runtime-constrained or low-depth settings. Since the exact ground-state energy

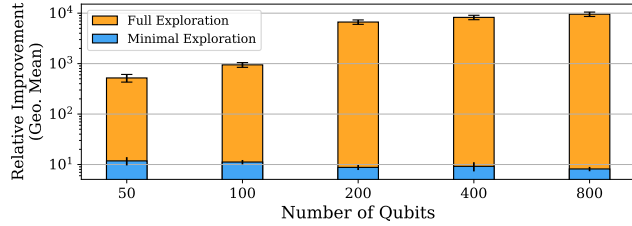


Figure 10. Relative Improvement evaluated on large 3-Regular Max-Cut instances.

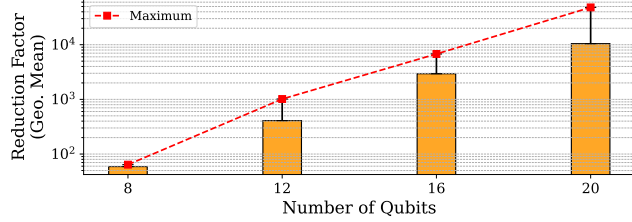


Figure 11. Factor of Reduction in Number of Initial Solution States in 3-Regular Max-Cut.

is intractable for these cases, this metric serves as a practical proxy for initialization quality.

5.3 Reduction in Solution Space with Initialization

To evaluate how effectively our initialization method narrows the solution search space, we compare the number of solution states explored by QAOA with SPIQ against random initialization. We perform this analysis on both the Knapsack problem and 3-regular Max-Cut instances across several medium-sized problem sizes.

To accurately estimate the distribution over solution states, we sample the initialized QAOA states 100 million times. As shown in Fig. 11, our initialization method achieves a maximum reduction of $48,132\times$ and an average reduction of $10,448\times$ in the number of solution states compared to random initialization on 3-regular Max-Cut instances.

Similarly, in Fig. 12, we observe strong reductions on the Knapsack instances, with a maximum reduction of $4,095\times$ and an average reduction of $789\times$ across the qubit sizes evaluated. Despite the added complexity of non-binary constraints and rugged energy landscapes, the initialization consistently concentrates amplitude into structured, low-energy regions of the solution space. Although the cause of the variability in Fig. 12 is not fully understood, these results collectively show that SPIQ allows QAOA to start from compact, high-quality regions across a wide range of combinatorial optimization problems.

5.4 Comparison Against Prior Work

In this subsection, we compare the performance of our initialization framework against prior warm-start techniques.

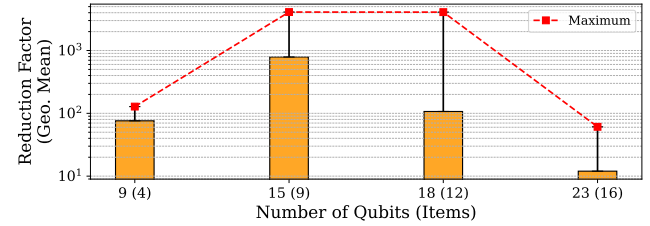


Figure 12. Factor of Reduction in Number of Initial Solution States in the Knapsack Problem.

Previous works have proposed problem-specific initialization methods to improve the convergence and solution quality of quantum optimization algorithms. Among these, Red-QAOA [64] is one of the leading warm-start approaches and serves as the primary baseline for our evaluation.

We evaluate the performance of Red-QAOA against our framework on both unweighted and weighted instances of Complete, 3-Regular, and Ego graphs. For each graph type, we select the best-performing initialization across 50 random restarts over 10 graph instances in a noiseless setting.

As shown in Fig. 13, we illustrate results for weighted graph instances while varying the *node reduction factor* in Red-QAOA. The node reduction factor quantifies the degree to which the graph’s size (in terms of nodes) decreases through the reduction process, directly influencing the feasibility of executing the resulting circuit on a smaller QPU. We observe that our framework consistently outperforms Red-QAOA across all graph types and node reduction factors. Specifically, while Red-QAOA achieves a maximum accuracy of approximately 60%, our framework reaches 99.9% accuracy, as discussed in greater detail in Subsection 5.1.1.

We further compare the performance of SPIQ on unweighted graph instances, as originally evaluated in the Red-QAOA study, illustrated in Fig. 14. Although Red-QAOA performs better on unweighted than on weighted graphs, our framework still achieves significantly higher accuracy across all configurations.

Finally, we note a key limitation of graph-specific warm-start methods like Red-QAOA. These rely on reduced graph representations to preserve the QAOA landscape, but for PCBO problems such as Knapsack, which lack a natural graph structure, any graph encoding is artificial and non-canonical. This provides no guarantee that the landscape is preserved, limiting Red-QAOA’s applicability beyond graph-based problems.

Overall, our results demonstrate that while Red-QAOA remains effective within its intended problem class, its reliance on graph-reducible formulations constrains its generality. In contrast, our initialization framework exhibits robust performance across diverse problem structures, highlighting its broader applicability.

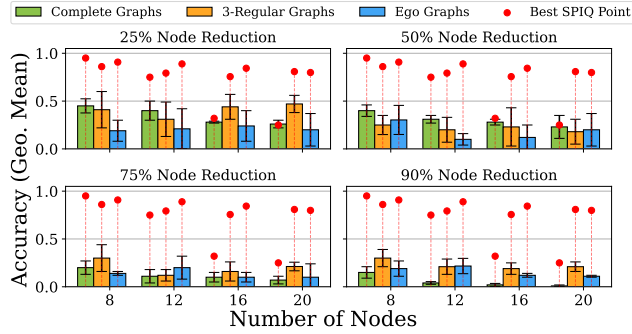


Figure 13. Performance of our framework against Red-QAOA on weighted Max-Cut instances

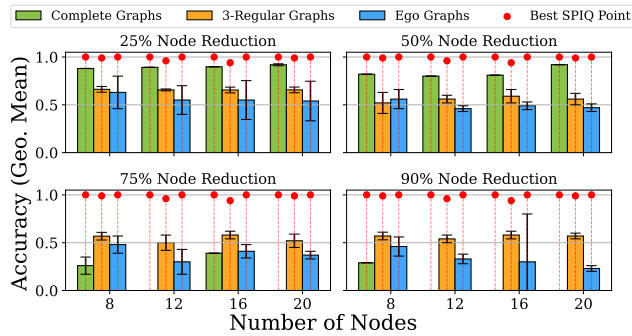


Figure 14. Performance of our framework against Red-QAOA on unweighted Max-Cut instances

5.5 Post-Initialization QAOA Exploration

A key factor in QAOA performance is effective exploration of the parameter space after initialization. Near- and intermediate-term devices are prone to noise, and rugged, plateau-filled landscapes can stall optimization [38]. Our framework addresses this by selecting high-quality initial points from SPIQ, providing robust starting states that mitigate challenges from device noise and landscape non-convexity.

We benchmark tuning trajectories initialized from SPIQ against both Red-QAOA and randomly selected starting points across several representative instances, as shown in Fig. 15. To ensure coverage of diverse landscape regions, we employ both the Gradient-Norm and Fixed-Interval selection methods to extract candidate points from SPIQ. We present both ideal and noisy simulations for a wide-range of problems.

For the 12-qubit weighted Max-Cut instance on a 3-regular graph, the point selected via SPIQ’s Gradient-Norm technique yields the highest-quality solution among all methods. In contrast, Red-QAOA plateaus after only a few hundred iterations, converging to a low-quality solution. Even the best point selected by SPIQ’s Fixed-Interval method eventually

stalls, underscoring the need for more advanced, landscape-adaptive SPIQ selection strategies.

On constrained instances, including Knapsack and the medical-dataset problem, we similarly find that SPIQ’s Clifford-derived initializations achieve substantially better solutions than random initialization, demonstrating the robustness of SPIQ across problem classes. We also note that Red-QAOA cannot be used for our non-graph benchmarks, as its procedure applies only to graph-structured problems; reformulating tasks like Knapsack or high-order interaction models into equivalent graphs is nontrivial and introduces additional modeling overhead that is beyond the scope of this work.

We further evaluate performance in a noisy regime using a depolarizing channel with a single-qubit error rate of 10^{-4} and a two-qubit error rate of 10^{-3} on unweighted Max-Cut problems on 3-regular graphs. In the 10-qubit example, one of the SPIQ points selected via the Fixed-Interval method successfully avoids the non-convex region that traps all other initializations, including Red-QAOA and random starts. We note that in the 12-qubit example, although both SPIQ and random initialization eventually reach the same solution, our K-GAPS method accelerates convergence. While faster convergence is not universally guaranteed, this result indicates that the K-GAPS method effectively increases the likelihood of choosing initial points located near high-quality regions of the landscape while avoiding proximity to non-convex or poorly conditioned areas, enhancing the efficiency and reliability of the optimization process.

This result further highlights the importance of multi-start initialization, especially in the presence of noise, where navigating the landscape becomes even more challenging, and selecting a diverse set of high-quality starting points becomes crucial for consistently reaching competitive solutions.

While this work does not focus on quantum space exploration (which depends on problem landscape, optimizer design, and device noise) Clifford search remains essential for rapid, reliable convergence, with benefits that scale for larger problems. On noisy devices, SPIQ initialization provides targeted starting points that reduce susceptibility to noise and barren plateaus, enabling faster convergence. Additionally, minimizing repeated quantum executions offers substantial economic savings, as prior studies [24] show variational algorithms on cloud platforms can become prohibitively costly even for modest problem sizes.

6 Discussion

Initialization Beyond Max-Cut-Specific Approaches: Prior QAOA initialization methods, including Red-QAOA [64] and Angle Rounding [67], have focused primarily on

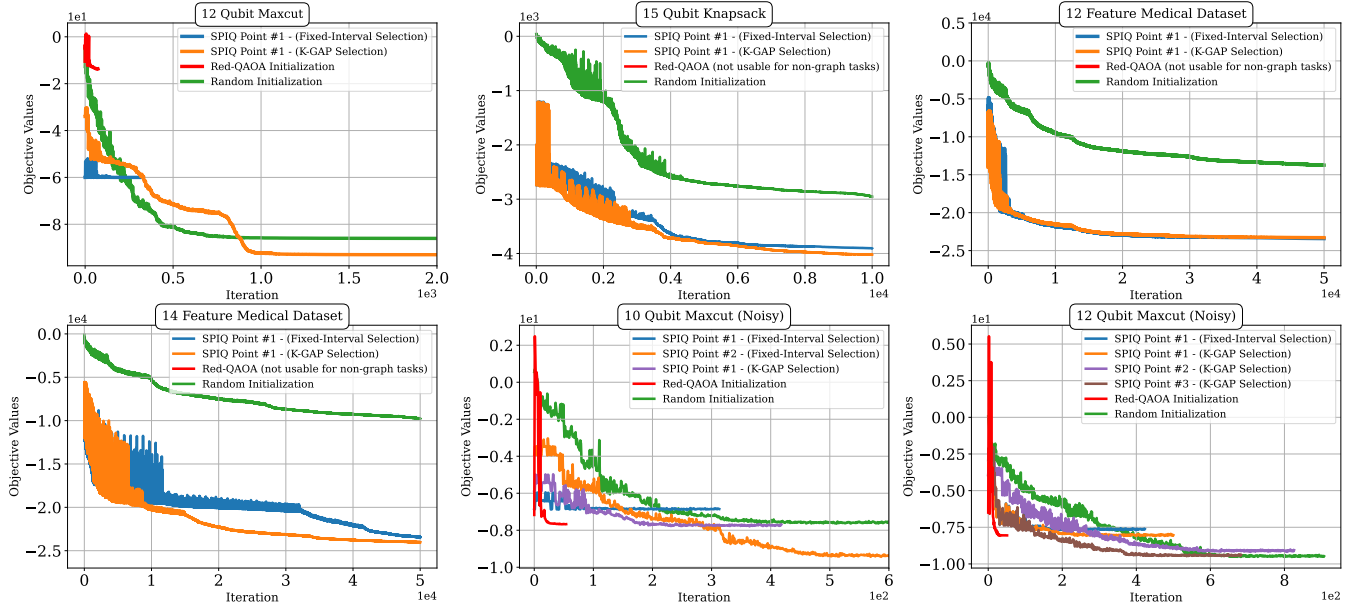


Figure 15. Effect of initialization choice on tuning across diverse problem instances.

Max-Cut, using instance-specific heuristics to identify promising regions of parameter space. While effective in these settings, they can incur significant classical overhead, and generalize poorly to broader weighted or large-scale problems, limiting their applicability beyond Max-Cut-like instances. Our framework addresses this gap, supporting a broader range of problem instances, including weighted and practically relevant combinatorial problems, beyond the unweighted Max-Cut.

Multi-Start for Efficient Exploration: Optimizing VQA circuits involves navigating rugged landscapes with many local optima [38], making careful initialization essential. We employ a multi-start approach with two selection techniques to sample diverse regions of the parameter space, reducing reliance on any single starting point. While K-GAPS considers landscape steepness, we note it is not universally superior to the Fixed-Interval method, highlighting the problem-dependent balance between exploration and exploitation. Nonetheless, K-GAPS is valuable for enforcing spatial diversity and identifying degenerate optima. Our results show multi-start strategies shape landscape coverage, with optimizers favoring different regions, as in Fig. 15.

Classical Optimization and Resource Scaling: We implement the Clifford search using a genetic algorithm to balance global exploration with robustness to noisy evaluations. More sophisticated optimizers could improve performance, but their classical cost remains small compared to QAOA circuit executions. Increasing classical resources mainly enables deeper and broader searches, making optimizer choice and resource allocation important for scaling initialization to larger or more complex problems.

Relevance in Fault-Tolerant Devices: Although VQAs are often associated with NISQ devices, QAOA and related algorithms remain relevant for intermediate and early fault-tolerant (EFT) machines, where efficient use of quantum resources is still crucial [12, 34]. Our framework, SPIQ, operates at a high level of abstraction and is agnostic to the underlying gateset (e.g., Clifford+ T or Clifford+ R_Z), enabling it to deliver the same initialization benefits on EFT and future fully fault-tolerant systems.

Future Work: Several directions emerge naturally from our study. A systematic study of multi-start strategies could clarify how to best balance global exploration with local refinement, especially with diverse optimizers. Expanding benchmarks beyond Max-Cut-like instances to more application-oriented problems would further test the robustness of our framework. Adapting parameter transfer techniques [18] to handle weighted or structured instances remains an open challenge.

7 Conclusion

We introduce an initialization framework that leverages the relaxed ma-QAOA ansatz to efficiently identify high-quality Clifford states as QAOA starting points, improving solution quality and reducing resource costs. We demonstrate its effectiveness across a range of problems, including Max-Cut, Knapsack, and real-world medical high-order interaction datasets, consistently achieving higher overlap with the ground-state energy. Our study provides multiple insights, including exploring advanced optimizers for noisy settings, refining initialization for complex instances, and scaling QAOA to larger, practical problem domains.

Acknowledgements

We thank Teague Tomesh and Frederic Chong for helpful and insightful discussions. This material is based upon work supported by the U.S. Department of Energy, Office of Science, Office of Advanced Scientific Computing Research, Accelerated Research in Quantum Computing under Award Number DE-SC0025633. This research used resources of the National Energy Research Scientific Computing Center, a DOE Office of Science User Facility supported by the Office of Science of the U.S. Department of Energy under Contract No. DE-AC02-05CH11231 using NERSC award ASCR-ERCAP0033197 and NERSC DDR-ERCAP0035341.

References

- [1] Tanweer Alam, Shamimul Qamar, Amit Dixit, and Mohamed Benaida. 2020. Genetic Algorithm: Reviews, Implementations, and Applications. *arXiv:2007.12673 [cs.OH]* <https://arxiv.org/abs/2007.12673>
- [2] Martin Anthony, Endre Boros, Yves Crama, and Arifan Gruber. 2017. Quadratization of higher degree pseudo-Boolean functions. In *International Conference on Integer Programming and Combinatorial Optimization*. Springer, 458–469. doi:10.1007/978-3-319-59250-3_37
- [3] Boaz Barak, Ankur Moitra, Ryan O'Donnell, Prasad Raghavendra, Oded Regev, David Steurer, Luca Trevisan, Aravindan Vijayaraghavan, David Witmer, and John Wright. 2015. Beating the random assignment on constraint satisfaction problems of bounded degree. *arXiv* (Aug. 2015). doi:10.48550/arXiv.1505.03424
- [4] Jacob Biamonte, Peter Wittek, Nicola Pancotti, Patrick Rebentrost, Nathan Wiebe, and Seth Lloyd. 2017. Quantum machine learning. *Nature* 549, 7671 (2017), 195–202.
- [5] Kostas Blekos, Dean Brand, Andrea Ceschini, Chiao-Hui Chou, Rui-Hao Li, Komal Pandya, and Alessandro Summer. 2024. A review on quantum approximate optimization algorithm and its variants. *Physics Reports* 1068 (2024), 1–66.
- [6] Endre Boros and Peter L. Hammer. 2002. Pseudo-boolean optimization. *Discrete Applied Mathematics* 123, 1–3 (2002), 155–225. doi:10.1016/S0166-218X(01)00341-9
- [7] Endre Boros, Peter L Hammer, and Gabriel Tavares. 2007. Local search heuristics for quadratic unconstrained binary optimization (QUBO). *Journal of Heuristics* 13, 2 (2007), 99–132.
- [8] M. Cerezo, Andrew Arrasmith, Ryan Babbush, Simon C. Benjamin, Suguru Endo, Keisuke Fujii, Jarrod R. McClean, Kosuke Mitarai, Xiao Yuan, Lukasz Cincio, and Patrick J. Coles. 2021. Variational Quantum Algorithms. *Nature Reviews Physics* 3, 9 (Aug. 2021), 625–644. doi:10.1038/s42254-021-00348-9
- [9] M. H. Cheng, K. E. Khosla, C. N. Self, M. Lin, B. X. Li, A. C. Medina, and M. S. Kim. 2022. Clifford Circuit Initialisation for Variational Quantum Algorithms. *arXiv:2207.01539 [quant-ph]* <https://arxiv.org/abs/2207.01539>
- [10] Chi-Ning Chou, Peter J. Love, Juspreet Singh Sandhu, and Jonathan Shi. 2022. Limitations of Local Quantum Algorithms on Random Max-k-XOR and Beyond. doi:10.48550/arXiv.2108.06049
- [11] Wim van Dam, Karim Eldefrawy, Nicholas Genise, and Natalie Parham. 2021. Quantum Optimization Heuristics with an Application to Knapsack Problems. In *2021 IEEE International Conference on Quantum Computing and Engineering (QCE)*. 160–170. doi:10.1109/QCE52317.2021.00033
- [12] Siddharth Dangwal, Suhas Vittal, Lennart Maximilian Seifert, Frederic T. Chong, and Gokul Subramanian Ravi. 2025. Variational Quantum Algorithms in the era of Early Fault Tolerance. *arXiv:2503.20963 [quant-ph]* <https://arxiv.org/abs/2503.20963>
- [13] E. Farhi, J. Goldstone, and S. Gutmann. 2015. A Quantum Approximate Optimization Algorithm Applied to a Bounded Occurrence Constraint Problem. *arXiv* (June 2015). doi:10.48550/arXiv.1412.6062
- [14] Edward Farhi, Jeffrey Goldstone, and Sam Gutmann. 2014. A Quantum Approximate Optimization Algorithm. doi:10.48550/arXiv.1411.4028
- [15] Edward Farhi, Jeffrey Goldstone, Sam Gutmann, and Leo Zhou. 2022. The Quantum Approximate Optimization Algorithm and the Sherrington-Kirkpatrick Model at Infinite Size. *Quantum* 6 (July 2022), 759. doi:10.22331/q-2022-07-07-759
- [16] Austin G. Fowler, Matteo Mariantoni, John M. Martinis, and Andrew N. Cleland. 2012. Surface codes: Towards practical large-scale quantum computation. *Physical Review A* 86, 3 (sep 2012). doi:10.1103/physreva.86.032324
- [17] Ahmed Fawzy Gad. 2021. PyGAD: An Intuitive Genetic Algorithm Python Library. *arXiv:2106.06158 [cs.NE]* <https://arxiv.org/abs/2106.06158>
- [18] Alexey Galda, Xiaoyuan Liu, Danylo Lykov, Yuri Alexeev, and Ilya Safro. 2021. Transferability of optimal QAOA parameters between random graphs. In *2021 IEEE International Conference on Quantum Computing and Engineering (QCE)*. 171–180. doi:10.1109/QCE52317.2021.00034
- [19] Fuchang Gao and Lixing Han. 2012. Implementing the Nelder-Mead simplex algorithm with adaptive parameters. *Comput. Optim. Appl.* 51, 1 (Jan. 2012), 259–277. doi:10.1007/s10589-010-9329-3
- [20] Fred Glover, Gary Kochenberger, and Yu Du. 2019. A tutorial on formulating and using QUBO models. *arXiv preprint arXiv:1811.11538* (2019). <https://arxiv.org/abs/1811.11538>
- [21] Google. [n. d.]. Google Quantum Computing Roadmap. <https://quantumai.google/roadmap>. Accessed: 2024-11-22.
- [22] Daniel Gottesman. 1998. The Heisenberg representation of quantum computers. *arXiv preprint quant-ph/9807006* (1998).
- [23] Lov K Grover. 1996. A fast quantum mechanical algorithm for database search. In *Proceedings of the twenty-eighth annual ACM symposium on Theory of computing*. 212–219.
- [24] Andi Gu, Angus Lowe, Pavel A Dub, Patrick J Coles, and Andrew Arrasmith. 2021. Adaptive shot allocation for fast convergence in variational quantum algorithms. *arXiv preprint arXiv:2108.10434* (2021).
- [25] Gurobi Optimization, LLC. 2024. Gurobi Optimizer Reference Manual. <https://www.gurobi.com>
- [26] Stuart Hadfield, Zhihui Wang, Bryan O'Gorman, Eleanor G. Rieffel, Davide Venturelli, and Rupak Biswas. 2019. From the Quantum Approximate Optimization Algorithm to a Quantum Alternating Operator Ansatz. *Algorithms* 12, 2 (Feb. 2019), 34. doi:10.3390/a12020034
- [27] M. B. Hastings. 2019. Classical and Quantum Bounded Depth Approximation Algorithms. *arXiv* (Aug. 2019). doi:10.48550/arXiv.1905.07047
- [28] Rebekah Herrman, Phillip C. Lotshaw, James Ostrowski, Travis S. Humble, and George Siopsis. 2021. Multi-angle Quantum Approximate Optimization Algorithm. *arXiv:2109.11455 [quant-ph]* <https://arxiv.org/abs/2109.11455>
- [29] IBM. [n. d.]. IBM Quantum Computing Roadmap. <https://www.ibm.com/roadmaps/quantum>. Accessed: 2024-11-22.
- [30] IBM. 2024. IBM ILOG CPLEX Optimization Studio. <https://www.ibm.com/products/ilog-cplex-optimization-studio>.
- [31] J. Preskill. 2025. Beyond NISQ: The Megauop Machine. *ACM Transactions on Quantum Computing* 6, 3 (April 2025), 1–7. doi:10.1145/3723153
- [32] Ali Javadi-Abhari, Matthew Treinish, Kevin Krsulich, Christopher J. Wood, Jake Lishman, Julien Gacon, Simon Martiel, Paul D. Nation, Lev S. Bishop, Andrew W. Cross, Blake R. Johnson, and Jay M. Gambetta. 2024. Quantum computing with Qiskit. *arXiv:2405.08810 [quant-ph]* <https://arxiv.org/abs/2405.08810>
- [33] Abhinav Kandala, Antonio Mezzacapo, Kristan Temme, Maika Takita, Markus Brink, Jerry M Chow, and Jay M Gambetta. 2017. Hardware-efficient variational quantum eigensolver for small molecules and

quantum magnets. *Nature* 549, 7671 (2017), 242–246.

[34] Amara Katabarwa, Katerina Gratsea, Athena Caesura, and Peter D. Johnson. 2024. Early Fault-Tolerant Quantum Computing. *PRX Quantum* 5 (Jun 2024), Issue 2. doi:10.1103/PRXQuantum.5.020101

[35] Youngseok Kim, Andrew Eddins, Sajant Anand, Ken Xuan Wei, Ewout Van Den Berg, Sami Rosenblatt, Hasan Nayfeh, Yantao Wu, Michael Zaletel, Kristan Temme, and Abhinav Kandala. 2023. Evidence for the utility of quantum computing before fault tolerance. *Nature* 618, 7965 (2023), 500–505.

[36] Diederik P. Kingma and Jimmy Ba. 2017. Adam: A Method for Stochastic Optimization. arXiv:1412.6980 [cs.LG] <https://arxiv.org/abs/1412.6980>

[37] Gary Kochenberger, Jin-Kao Hao, Fred Glover, Mark Lewis, Zhipeng Lü, Haibo Wang, and Yang Wang. 2014. The unconstrained binary quadratic programming problem: a survey. *Journal of Combinatorial Optimization* 28 (2014), 58–81. doi:10.1007/s10878-014-9734-0

[38] Martín Larocca, Supanut Thanasilp, Samson Wang, Kunal Sharma, Jacob Biamonte, Patrick J. Coles, Lukasz Cincio, Jarrod R. McClean, Zoë Holmes, and M. Cerezo. 2025. Barren plateaus in variational quantum computing. *Nature Reviews Physics* 7, 4 (March 2025), 174–189. doi:10.1038/s42254-025-00813-9

[39] Xinwei Lee, Ningyi Xie, Dongsheng Cai, Yoshiyuki Saito, and Nobuyoshi Asai. 2023. A Depth-Progressive Initialization Strategy for Quantum Approximate Optimization Algorithm. *Mathematics* 11, 9 (2023), 2176. arXiv:2209.11348 [quant-ph] doi:10.3390/math11092176

[40] Xinwei Lee, Xinjian Yan, Ningyi Xie, Dongsheng Cai, Yoshiyuki Saito, and Nobuyoshi Asai. 2024. Iterative layerwise training for the quantum approximate optimization algorithm. *Physical Review A* 109, 5 (2024), 052406.

[41] Cedric Yen-Yu Lin and Yechao Zhu. 2016. Performance of QAOA on Typical Instances of Constraint Satisfaction Problems with Bounded Degree. *arXiv* (Jan. 2016). doi:10.48550/arXiv.1601.01744

[42] Andrew Lucas. 2014. Ising formulations of many NP problems. *Frontiers in Physics* 2 (2014), 5. doi:10.3389/fphy.2014.00005

[43] Kunal Marwaha. 2021. Local classical MAX-CUT algorithm outperforms $\$p=2\$$ QAOA on high-girth regular graphs. *Quantum* 5 (April 2021). doi:10.22331/q-2021-04-20-437

[44] K. Mitarai, M. Negoro, M. Kitagawa, and K. Fujii. 2018. Quantum circuit learning. *Phys. Rev. A* 98 (Sep 2018), 032309. Issue 3. doi:10.1103/PhysRevA.98.032309

[45] Nikolaj Moll, Panagiotis Barkoutsos, Lev Bishop, Jerry Chow, Andrew Cross, Daniel Egger, Stefan Filipp, Andreas Fuhrer, Jay Gambetta, Marc Ganzhorn, Abhinav Kandala, Antonio Mezzacapo, Peter Müller, Walter Riess, Gian Salis, John Smolin, Ivano Tavernelli, and Kristan Temme. 2018. Quantum optimization using variational algorithms on near-term quantum devices. *Quantum Science and Technology* 3 (06 2018). doi:10.1088/2058-9565/aab822

[46] Prakash Murali, Jonathan M Baker, Ali Javadi-Abhari, Frederic T Chong, and Margaret Martonosi. 2019. Noise-adaptive compiler mappings for noisy intermediate-scale quantum computers. In *Proceedings of the Twenty-Fourth International Conference on Architectural Support for Programming Languages and Operating Systems*. 1015–1029.

[47] National Energy Research Scientific Computing Center (NERSC). 2025. Perlmutter System. <https://www.nersc.gov/what-we-do/computing-for-science/perlmutter>. Accessed: 2025-11-17.

[48] Jorge Nocedal and Stephen J. Wright. 2006. *Numerical Optimization* (2 ed.). Springer.

[49] Julius Beneoluchi Odili. 2017. Combinatorial optimization in science and engineering. *Current Science* (2017), 2268–2274.

[50] Joe O’Gorman and Earl T. Campbell. 2017. Quantum computation with realistic magic-state factories. *Physical Review A* 95, 3 (Mar 2017). doi:10.1103/physreva.95.032338

[51] Alberto Peruzzo, Jarrod McClean, Peter Shadbolt, Man-Hong Yung, Xiao-Qi Zhou, Peter J Love, Alán Aspuru-Guzik, and Jeremy L O’brien. 2014. A variational eigenvalue solver on a photonic quantum processor. *Nature communications* 5 (2014), 4213.

[52] John Preskill. 2018. Quantum Computing in the NISQ era and beyond. *Quantum* 2 (2018), 79.

[53] Qiskit contributors. 2023. Qiskit: An Open-source Framework for Quantum Computing. doi:10.5281/zenodo.2573505

[54] Ronald L Rardin. 1998. *Optimization in operations research*. Vol. 166. Prentice Hall Upper Saddle River, NJ.

[55] Gokul Subramanian Ravi, Pranav Gokhale, Yi Ding, William M. Kirby, Kaitlin N. Smith, Jonathan M. Baker, Peter J. Love, Henry Hoffmann, Kenneth R. Brown, and Frederic T. Chong. 2023. CAFQA: A classical simulation bootstrap for variational quantum algorithms. In *ACM International Conference on Architectural Support for Programming Languages and Operating Systems (ASPLOS)*. doi:10.48550/ARXIV.2202.12924

[56] A. H. G. Rinnooy Kan and G. T. Timmer. 1987. Stochastic Global Optimization Methods Part I: Clustering Methods. *Mathematical Programming* 39 (1987), 27–56.

[57] Stefan H. Sack and Maksym Serbyn. 2021. Quantum annealing initialization of the quantum approximate optimization algorithm. *Quantum* 5 (July 2021), 491. doi:10.22331/q-2021-07-01-491

[58] Abdelkader Sbihi and Richard W Eglese. 2010. Combinatorial optimization and green logistics. *Annals of Operations Research* 175, 1 (2010), 159–175.

[59] Dhirpal Shah, Mariesa Teo, Ryan A. Robinett, Sophia Madejski, Zachary Morrell, Siddhi Ramesh, Colin Campbell, Bharath Thotakura, Victory Omole, Ben Hall, Aram W. Harrow, Teague Tomesh, Alexander T. Pearson, Frederic T. Chong, and Samantha J. Riesenfeld. 2025. Toward Quantum-Enabled Biomarker Discovery: An Outlook from Q4Bio. arXiv:2509.25904 [quant-ph] <https://arxiv.org/abs/2509.25904>

[60] Peter W. Shor. 1997. Polynomial-Time Algorithms for Prime Factorization and Discrete Logarithms on a Quantum Computer. *SIAM J. Comput.* 26, 5 (Oct 1997), 1484–1509. doi:10.1137/s0097539795293172

[61] Kristina P. Sinaga and Miin-Shen Yang. 2020. Unsupervised K-Means Clustering Algorithm. *IEEE Access* 8 (2020), 80716–80727. doi:10.1109/ACCESS.2020.2988796

[62] James C. Spall. 1998. An Overview of the Simultaneous Perturbation Method for Efficient Optimization. *Johns Hopkins APL Technical Digest* 19, 4 (1998), 482–492.

[63] Michael Streif and Martin Leib. 2020. Training the quantum approximate optimization algorithm without access to a quantum processing unit. *IOP* 5, 3 (May 2020), 034008. doi:10.1088/2058-9565/ab8c2b Publisher: IOP Publishing.

[64] Meng Wang, Bo Fang, Ang Li, and Prashant J Nair. 2024. Red-qaoa: Efficient variational optimization through circuit reduction. In *Proceedings of the 29th ACM International Conference on Architectural Support for Programming Languages and Operating Systems, Volume 2*. 980–998.

[65] Samson Wang, Enrico Fontana, Marco Cerezo, Kunal Sharma, Akira Sone, Lukasz Cincio, and Patrick J Coles. 2020. Noise-induced barren plateaus in variational quantum algorithms. *arXiv preprint arXiv:2007.14384* (2020).

[66] Zhihui Wang, Stuart Hadfield, Zhang Jiang, and Eleanor G. Rieffel. 2018. Quantum Approximate Optimization Algorithm for MaxCut: A Fermionic View. *Physical Review A* 97, 2 (Feb. 2018), 022304. doi:10.1103/PhysRevA.97.022304

[67] Anthony Wilkie, James Ostrowski, and Rebekah Herrman. 2024. An angle rounding parameter initialization technique for ma-QAOA. *arXiv preprint arXiv:2404.10743* (2024).

[68] Z. Zhang. 2023. PRIMA: Reference Implementation for Powell’s Methods with Modernization and Amelioration. available at <http://www.libprima.net>, DOI: 10.5281/zenodo.8052654.

[69] Leo Zhou, Sheng-Tao Wang, Soonwon Choi, Hannes Pichler, and Mikhail D. Lukin. 2020. Quantum Approximate Optimization Algorithm: Performance, Mechanism, and Implementation on Near-Term Devices. *Phys. Rev. X* 10 (Jun 2020), 021067. Issue 2. doi:10.1103/PhysRevX.10.021067

[70] Ciyou Zhu, Richard H. Byrd, Peihuang Lu, and Jorge Nocedal. 1997. Algorithm 778: L-BFGS-B: Fortran subroutines for large-scale bound-constrained optimization. *ACM Trans. Math. Softw.* 23, 4 (Dec. 1997), 550–560. doi:10.1145/279232.279236

[71] Zoltán Zimborás, Bálint Koczor, Zoë Holmes, Elsi-Mari Borrelli, András Gilyén, Hsin-Yuan Huang, Zhenyu Cai, Antonio Acín, Leandro Aolita, Leonardo Banchi, Fernando G. S. L. Brandão, Daniel Cavalcanti, Toby Cubitt, Sergey N. Filippov, Guillermo García-Pérez, John Goold, Orsolya Kálmán, Elica Kyoseva, Matteo A. C. Rossi, Boris Sokolov, Ivano Tavernelli, and Sabrina Maniscalco. 2025. Myths around quantum computation before full fault tolerance: What no-go theorems rule out and what they don’t. arXiv:2501.05694 [quant-ph] <https://arxiv.org/abs/2501.05694>